Electronic Supplementary Information

Performance of second generation ICP-TOFMS for (multi-)isotope ratio analysis: A case study on B, Sr and Pb and their isotope fractionation behavior during the measurements

Anika Retzmann[1,2*], Sebastian Faßbender[1*], Martin Rosner[3], Marcus von der Au[1], Jochen Vogl[1]

*These two authors contributed equally as main authors to the presented work

corresponding author

Anika Retzmann (anika.retzmann@bam.de, anika.retzmann@ucalgary.ca)

[1] Bundesanstalt für Materialforschung und -prüfung, Division 1.1 – Inorganic Trace Analysis, Richard-Willstätter-Str. 11, 12489 Berlin, Germany

[2] University of Calgary – Department of Physics and Astronomy, 2500 University Dr. NW, Calgary, AB T2N 1N4, Canada

[3] IsoAnalysis UG, Berlin, Germany

Table S1 Overview of isotopic analysis using prototype ICP-TOFMS, first generation ICP-TOFMS with a secondary electron multiplier (SEM) and second generation ICP-TOFMS with a micro-channel plate (MCP). For this overview table, only isotopic analysis using ICP-TOFMS in standard set-up (no hyphenation) were considered. The authors do not claim that this overview table is complete.

Prototype ICP-TOFMS							
Isotopic System	**Precision – RSD (%)**	**Integration Time**	**# of Runs (*M*)**	**IIF per mass unit (%) ***	**Instrument**	**Detection**	**Reference**
$^{107}Ag/^{109}Ag$	0.56	10 s	-	-	Prototype ICP-TOFMS[1]	MCP	[2]
$^{90}Zr/^{91}Zr$	0.51	10 min	-	4.3	Prototype ICP-TOFMS[1]	MCP	[3]
$^{94}Zr/^{90}Zr$	0.27			-3.7			
$^{107}Ag/^{109}Ag$	0.22			-1.1			
$^{110}Cd/^{114}Cd$	0.59			-1.8			
$^{112}Cd/^{114}Cd$	0.57			-0.7			
$^{121}Sb/^{123}Sb$	0.36			-2.2			
$^{143}Nd/^{142}Nd$	0.39			0.6			
$^{144}Nd/^{142}Nd$	0.28			-0.9			
$^{63}Cu/^{65}Cu$	0.031	30 s	10	-	Prototype axial ICP-TOFMS (Leco Renaissance)	SEM – analog mode	[4]
$^{64}Zn/^{66}Zn$	0.056			-			
$^{86}Sr/^{87}Sr$	0.044			-			
$^{86}Sr/^{88}Sr$	0.038			-			
$^{107}Ag/^{109}Ag$	0.033			-			
$^{137}Ba/^{138}Ba$	0.051			-			
$^{204}Pb/^{208}Pb$	0.069			-			
$^{206}Pb/^{207}Pb$	0.023			0.1			
$^{206}Pb/^{208}Pb$	0.041			-0.2			
1st Generation ICP-TOFMS							
Isotopic System*	**Precision – RSD (%)**	**Integration Time**	**# of Runs (*M*)**	**IIF per mass unit (%) ****	**Instrument**	**Detection**	**Reference**
$^{25}Mg/^{24}Mg$	0.07	30 s	10	4.4	axial ICP-TOFMS (Leco Renaissance)	SEM – analog mode	[5]
$^{26}Mg/^{24}Mg$	0.09			5.1			

$^{85}Rb/^{87}Rb$	0.07			-1.2			
$^{194}Pt/^{195}Pt$	0.1			-1.5			
$^{198}Pt/^{195}Pt$	0.2			-0.8			
$^{6}Li/^{7}Li$	0.42	30 s	10	-12.8	axial ICP-TOFMS (Leco Renaissance)	SEM – analog mode	6
$^{25}Mg/^{24}Mg$	0.072			4.3			
$^{26}Mg/^{24}Mg$	0.095			4.2			
$^{85}Rb/^{87}Rb$	0.072			-1.2			
$^{86}Sr/^{88}Sr$	0.033			-0.2			
$^{107}Ag/^{109}Ag$	0.039			1.8			
$^{111}Cd/^{114}Cd$	0.052			-0.9			
$^{112}Cd/^{114}Cd$	0.067			-1.4			
$^{136}Ba/^{138}Ba$	0.048			-0.7			
$^{137}Ba/^{138}Ba$	0.048			-1.0			
$^{194}Pt/^{195}Pt$	0.13			-1.5			
$^{198}Pt/^{195}Pt$	0.23			-0.8			
$^{206}Pb/^{208}Pb$	0.11			-0.2			
$^{207}Pb/^{208}Pb$	0.23			0.2			
$^{25}Mg/^{24}Mg$	0.04	50 s	10	Approx. 1%	orthogonal ICP-TOFMS (GBC Optimass8000)	SEM - pulse counting	7
$^{65}Cu/^{63}Cu$	0.26			-			
$^{107}Ag/^{109}Ag$	0.17			Approx. 0.12 %			
$^{140}Ce/^{142}Ce$	0.28			-			
$^{171}Yb/^{173}Yb$	0.16			-			
$^{195}Pt/^{194}Pt$	0.19			-			
$^{205}Tl/^{203}Tl$	0.25			-			
$^{235}U/^{238}U$	0.55			-			
$^{206}Pb/^{207}Pb$	<0.15	30	8	Approx. -0.5 to 0.2	axial ICP-TOFMS (Leco Renaissance)	SEM - pulse counting	8
$^{208}Pb/^{206}Pb$	<0.2			Approx. -1.2 to -0.8			
$^{206}Pb/^{204}Pb$	<1.8			Approx. -1.9 to -0.9			
$^{206}Pb/^{207}Pb$	<0.15	30	8	-	axial ICP-TOFMS (Leco Renaissance)	SEM - pulse counting	9
$^{208}Pb/^{206}Pb$	<0.18			-			

$^{207}Pb/^{208}Pb$	0.01			-			
$^{196}Hg/^{202}Hg$	-	-	-	7.6	axial ICP-TOFMS (Leco Renaissance)	SEM - pulse counting	[10]
$^{198}Hg/^{202}Hg$	-			-0.4			
$^{199}Hg/^{202}Hg$	0.39			-0.8			
$^{200}Hg/^{202}Hg$	0.30			0.9			
$^{201}Hg/^{202}Hg$	0.82			3.1			
$^{204}Hg/^{202}Hg$	-			0.9			
$^{200}Hg/^{201}Hg$	0.18	55 s	6	-	orthogonal ICP-TOFMS (GBC Optimass8000)	SEM – analog mode	[11]
$^{202}Hg/^{201}Hg$	0.26			-			
$^{11}B/^{10}B$	0.2	5 s	-	-	orthogonal ICP-TOFMS (GBC Optimass8000)	SEM	[12]
$^{207}Pb/^{206}Pb$	0.14	10 s	5	-	orthogonal ICP-TOFMS (GBC Optimass8000)	SEM – analog mode	[13]
$^{63}Cu/^{65}Cu$	0.28	10 s	10	Approx. -1.8 to 2.2	orthogonal ICP-TOFMS (GBC Optimass8000)	SEM – analog mode	[14]
$^{107}Ag/^{109}Ag$	0.28			Approx. -0.8			
$^{111}Cd/^{112}Cd$	0.51			Approx. -4.8 to 0.5			
$^{208}Pb/^{206}Pb$	0.26			Approx. -2.2 to 3.0			
2nd Generation ICP-TOFMS							
Isotopic System*	**Precision – RSD (%)**	**Integration Time**	**# of Runs (*M*)**	**IIF per mass unit (%) ****	**Instrument**	**Detection**	**Reference**
$^{109}Ag/^{107}Ag$	0.04	100 s	1000	Approx. -8.7	orthogonal ICP-TOFMS (TOFWERK icpTOF)	MCP	[15]
$^{153}Eu/^{151}Eu$	0.02			Approx. 4.6			
$^{63}Cu/^{65}Cu$	0.18	10 s	10	Approx. -7.6 to -6.5	orthogonal ICP-TOFMS (TOFWERK icpTOF)	MCP	[14]
$^{107}Ag/^{109}Ag$	0.084			Approx. -3.8 to -3.3			
$^{111}Cd/^{112}Cd$	0.14			Approx. -7.6 to -5.8			
$^{208}Pb/^{206}Pb$	0.57			Approx. 1			
$^{11}B/^{10}B$	0.14	10 s	20	-11.3 ± 1.7 (2 *s*, *N* = 40)	orthogonal ICP-TOFMS (TOFWERK icpTOF)	MCP	This study
$^{88}Sr/^{86}Sr$	0.12			-0.2 ± 3.3 (2 *s*, *N* = 30)			

$^{87}Sr/^{86}Sr$	0.15			2.2 ± 3.7 (2 *s*, *N* = 30)			
$^{206}Pb/^{204}Pb$	0.20			1.9 ± 1.3 (2 *s*, *N* = 30)			
$^{208}Pb/^{206}Pb$	0.07			4.5 ± 1.4 (2 *s*, *N* = 30)			
$^{207}Pb/^{206}Pb$	0.07			4.2 ± 1.6 (2 *s*, *N* = 30)			

* Calculated for isotope ratios of heavier isotope over lighter isotope in accordance to Heumann *et al*.[16] and Irrgeher & Prohaska[17] – used masses recommended by IUPAC/CIAAW.[18, 19]

Table S2 Instrumental settings of the ICP-TOFMS instruments used for isotope ratio analysis.

Parameter	**icpTOF 2R (TOFWERK)**
Nebulizer	Glass concentric, 200 µL/min, pumped
Spray chamber	Glass cyclonic, cooled to 2.7°C
Injector	2.5 mm
Sampling depth	4.5 mm
Power	1450 W
Nebulizer gas flow	Approx. 1.1 L/min
Auxiliary gas flow	0.8 L/min
Colling gas flow	14 L/min
CCT focus lens	3.65 V
CCT mass	110.09 V
CCT bias	-2.0 V
Collision cell gas	non
Notch 1	40 Th, 2 V
Notch 2	34.3 Th, 1.5 V
Notch 3	18 Th, 2.5 V
Notch 4	15.2 Th, 2 V
Notch bias	-17.8 V
Notch amplitude	Approx. 134 V
Data point per sample	400
Integration time	503 ms (N = 11000 extractions, 46 µs/extraction)
Acquisition time	10 s
Runs (M)	20
Isotopes of interest	^{10}B, ^{11}B, ^{84}Sr, ^{85}Rb, ^{86}Sr, ^{87}Sr (^{87}Rb), ^{88}Sr, ^{202}Hg, ^{203}Tl, ^{204}Pb (^{204}Hg), ^{205}Tl, ^{206}Pb, ^{207}Pb, ^{208}Pb

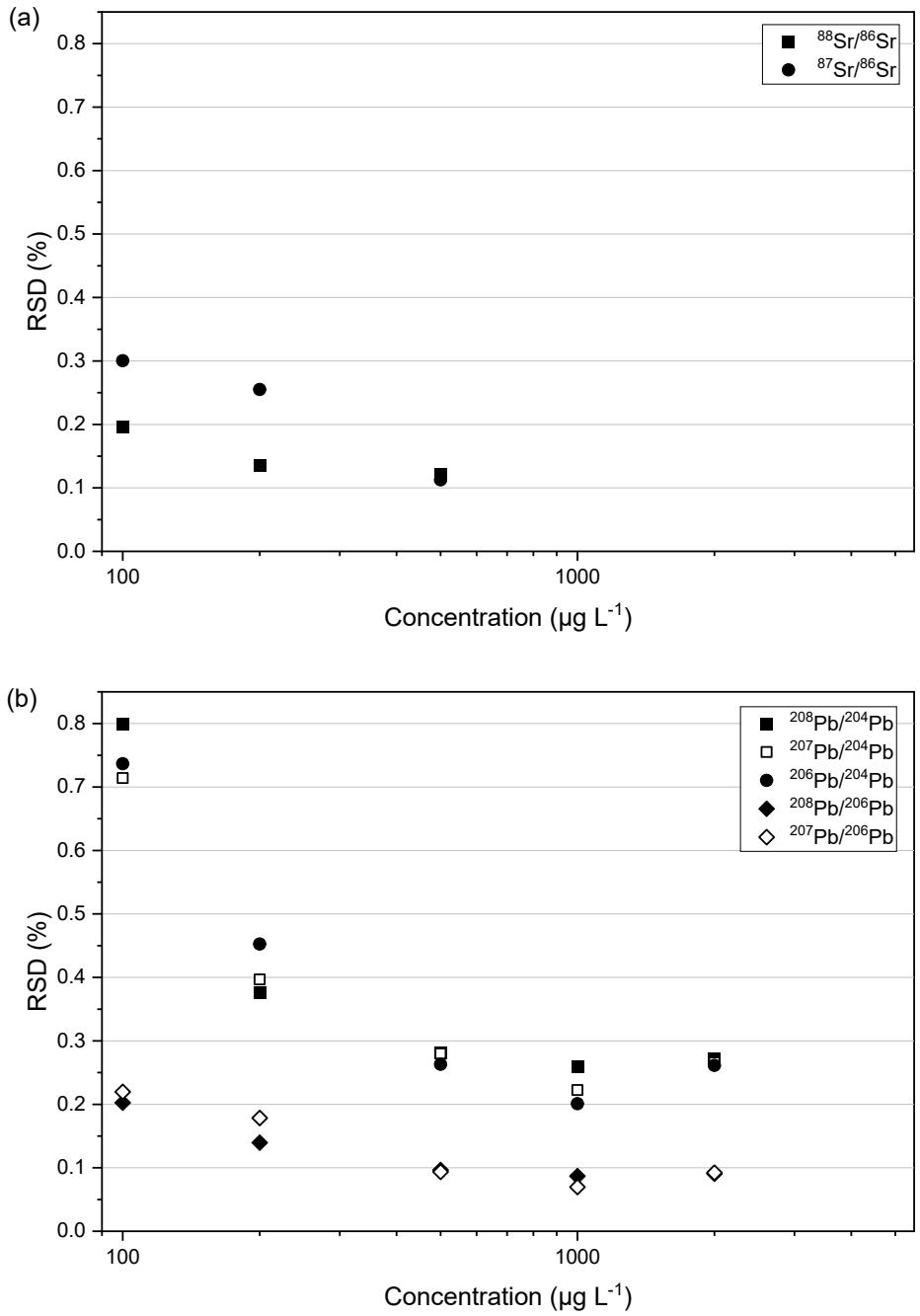

Figure S1 Isotope ratio precision of (a) Sr and (b) Pb – expressed as RSD (%) for an acquisition time of 10 s per run (M) and $M = 20$, obtained for different elemental mass concentrations. The data shown are from the measurement of a mixture in which B, Sr, and Pb were detected simultaneously.

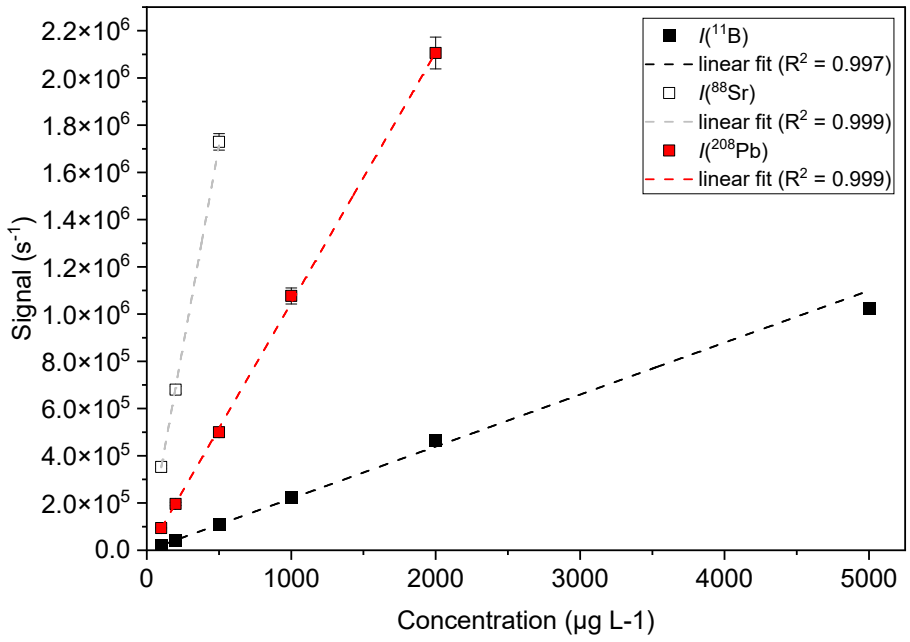

Figure S2 Linearity of the MCP detector observed for ^{11}B, ^{88}Sr and ^{208}Pb over a concentration range from 100 µg L^{-1} till 5000 µg L^{-1}. Calibration solutions contained B, Sr and Pb. Error bars correspond to 2 *s* (acquisition time of 0.5 s, $M = 400$).

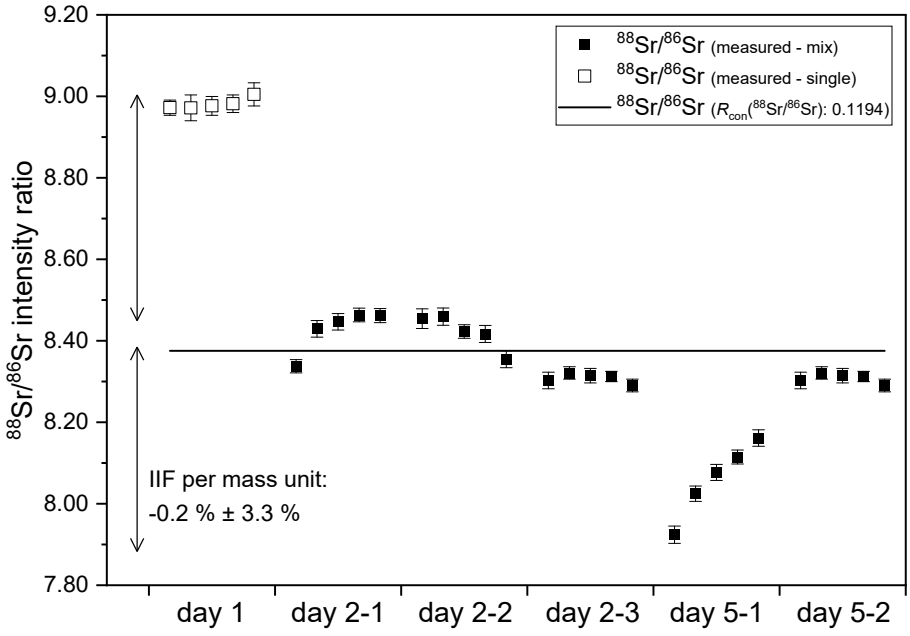

Figure S3 Intensity ratios of $^{88}Sr/^{86}Sr$ over a period of five days for 30 discontinuous measurements of NIST SRM 987. Error bars correspond to 2 *s* (acquisition time of 10 s, $M = 20$). The reported data are from measurements of both a single element solution and a mixture of B, Sr and Pb.

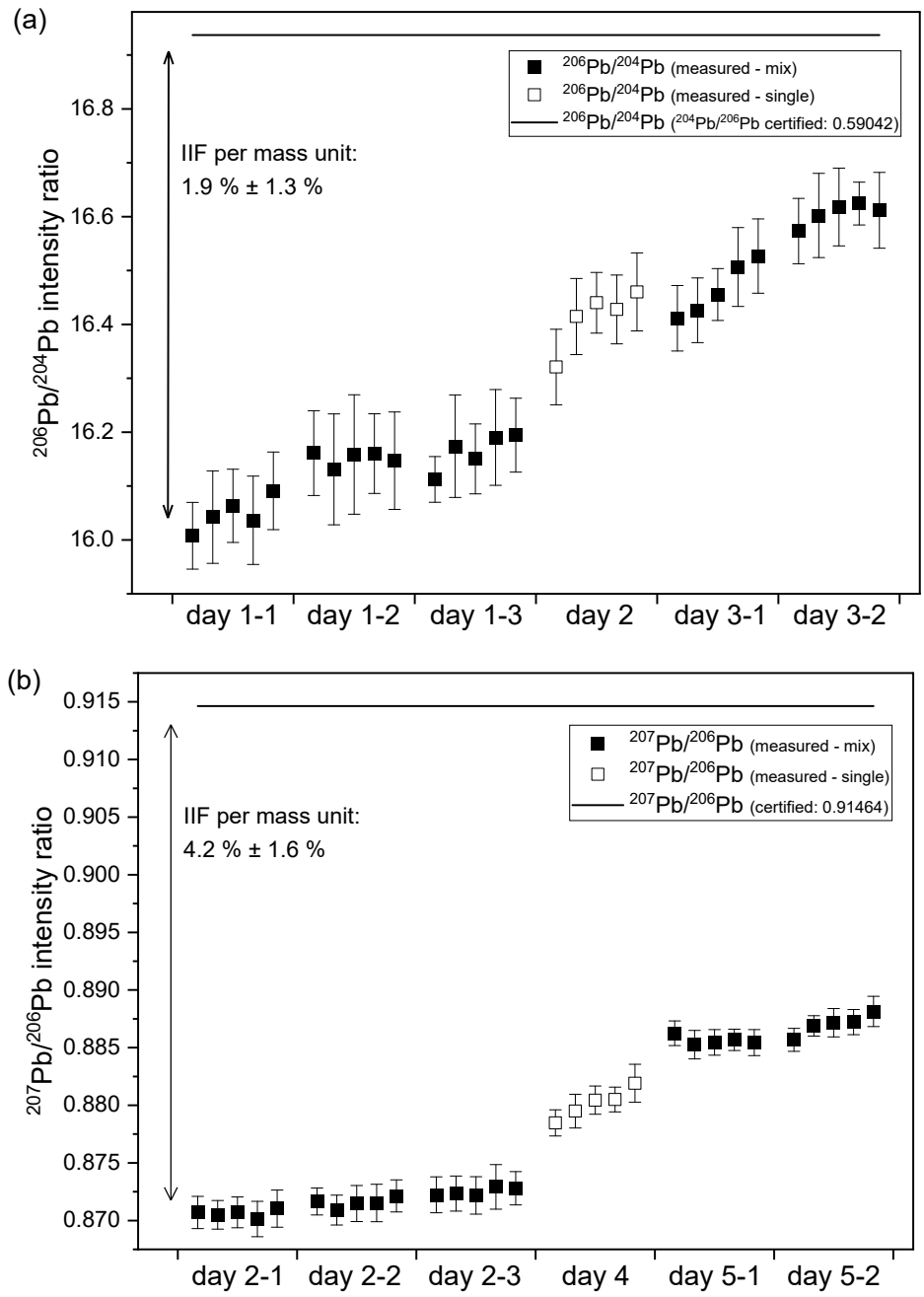

Figure S4 Intensity ratios of (a) $^{206}Pb/^{204}Pb$ and (b) $^{207}Pb/^{206}Pb$ over a period of five days for 30 discontinuous measurements of NIST SRM 987. Error bars correspond to 2 *s* (acquisition time of 10 s, $M = 20$). The reported data are from measurements of both a single element solution and a mixture of B, Sr and Pb.

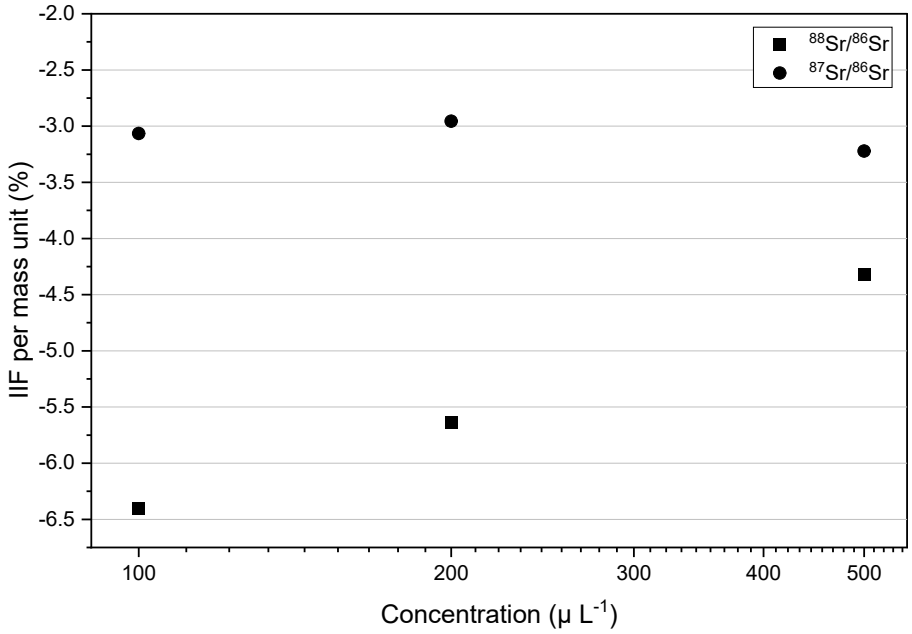

Figure S5 IIF per mass unit (%) of $^{87}Sr/^{86}Sr$ and $^{88}Sr/^{86}Sr$ intensity ratios as a function of mass concentration – 100 µg L^{-1} to 500 µg L^{-1}. Error bars correspond to 2 *s* (acquisition time of 10 s, *M* = 20). The data shown are from the measurement of a mixture in which B, Sr, and Pb were detected simultaneously.

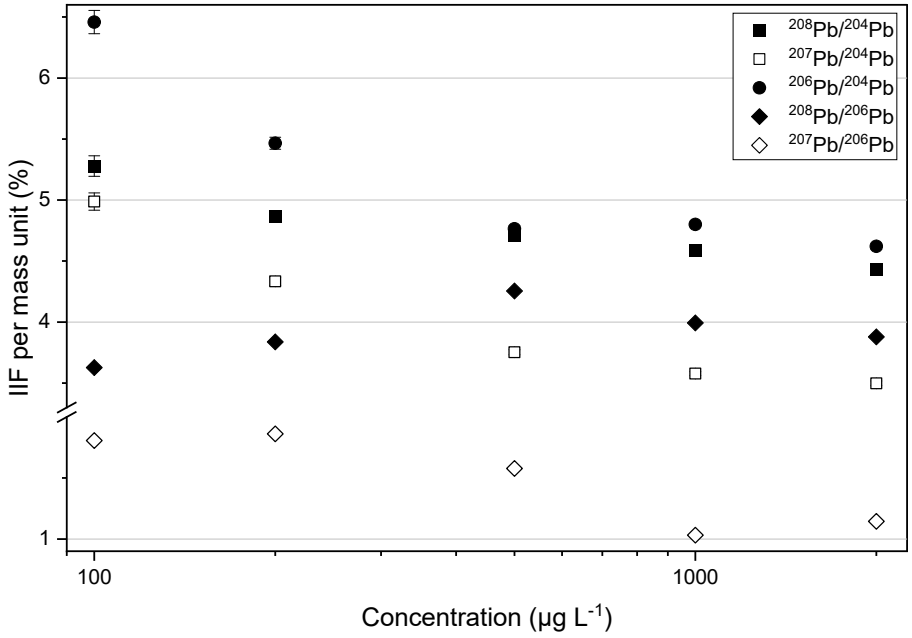

Figure S6 IIF per mass unit (%) of Pb intensity ratios as a function of mass concentration – 100 µg L^{-1} to 2000 µg L^{-1}. Error bars correspond to 2 *s* (acquisition time of 10 s, *M* = 20). The data shown are from the measurement of a mixture in which B, Sr, and Pb were detected simultaneously.

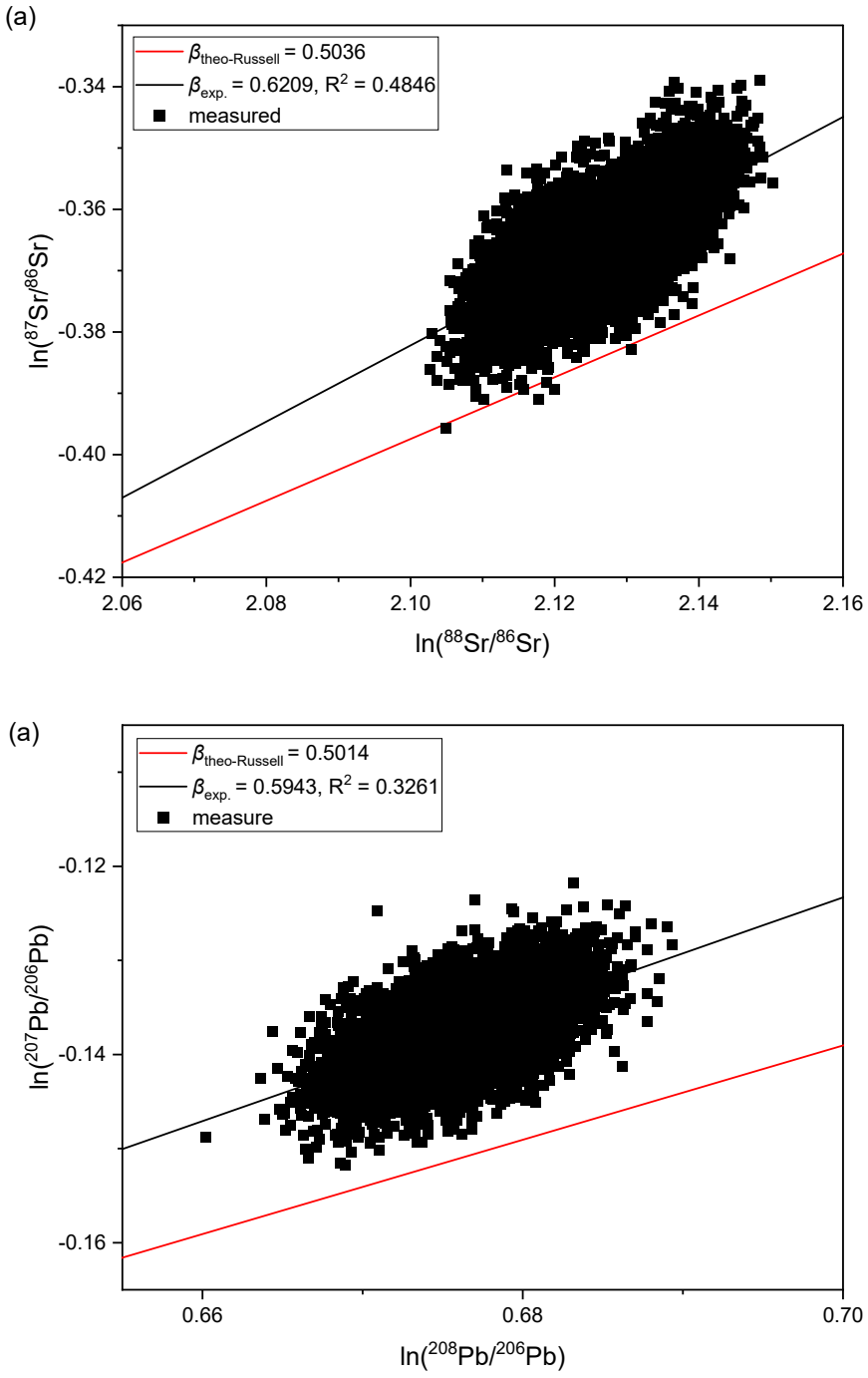

Figure S7 Three-isotope plot for (a) Sr and (b) Pb arising from 15 measurements over eight hours of NIST SRM 987 and NIST SRM 981 (integration time 0.5 s, M = 2000). Solid lines represent experimentally determined slope ($\beta_{exp.}$) and predicted mass-dependent fractionation line ($\beta_{theo\text{-}Russell}$). The data shown are from the measurement of a mixture in which B, Sr, and Pb were detected simultaneously.

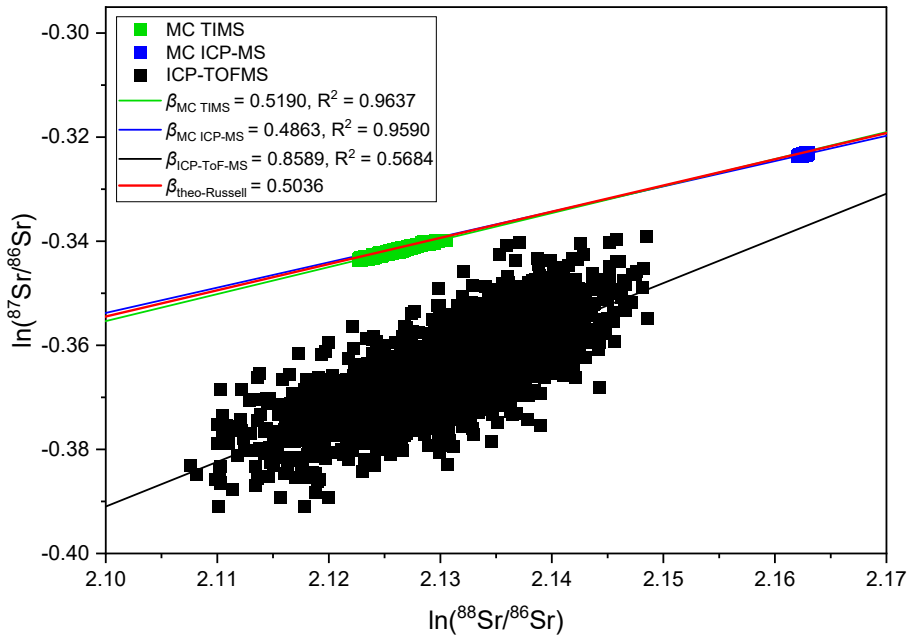

Figure S 8 Three-isotope plot for Sr from measurements over several hours of NIST SRM 987 using ICP-TOFMS (integration time 0.5 s, M = 2000), MC TIMS (integration time 24 s, M = 443) and MC ICP-MS (integration time 42 s, M = 238). Solid lines represent experimentally determined slopes ($\beta_{instrument}$) and predicted mass dependent fractionation line ($\beta_{theo-Russell}$). In case of ICP-TOFMS, the data shown are from the measurement of a **mixture** in which B, Sr, and Pb were detected simultaneously.

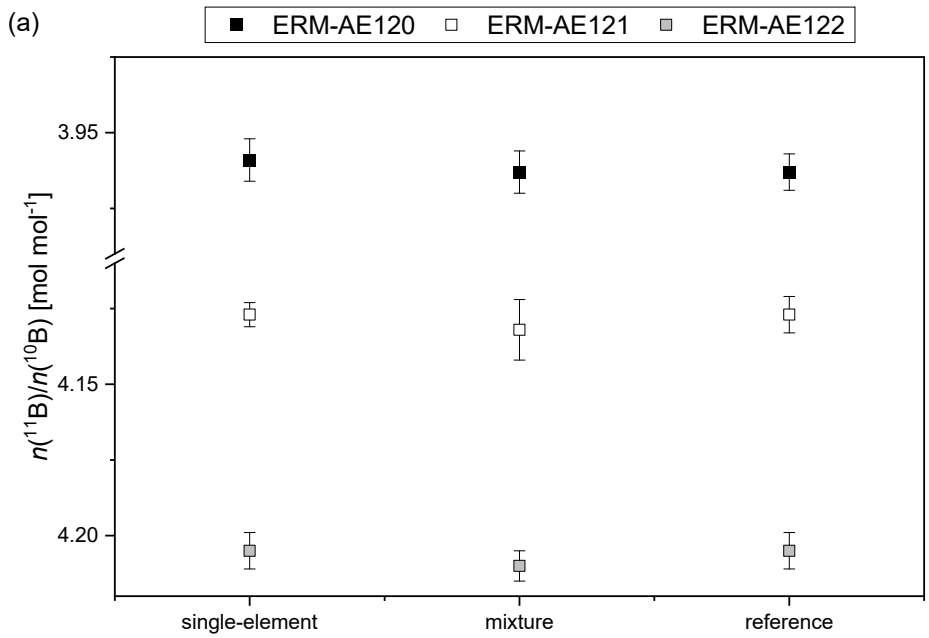

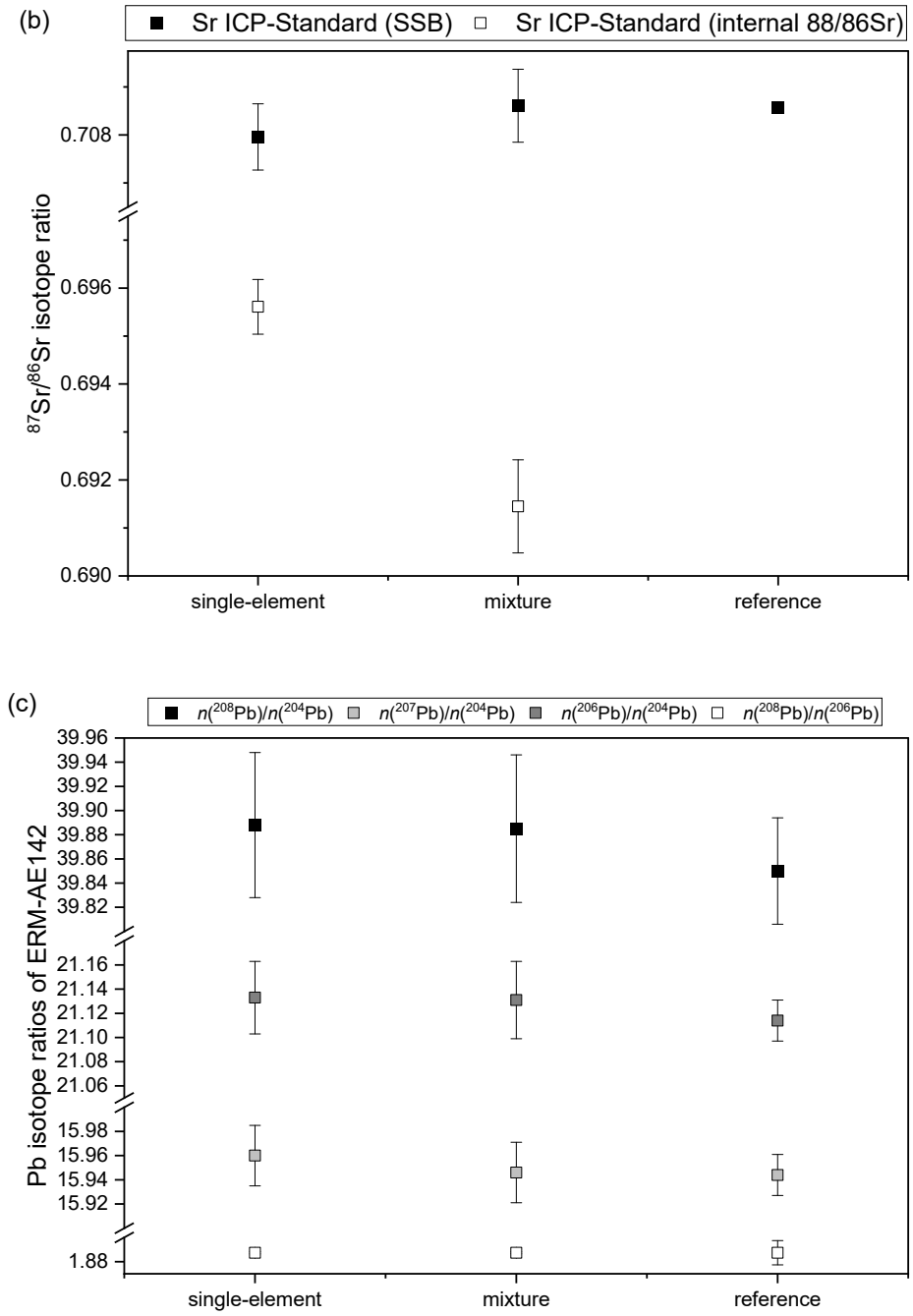

Figure S 9 (a) absolute $^{11}B/^{10}B$ isotope ratios of ERM-AE120, ERM-AE121 and ERM-AE122, (b) absolute and conventional $^{87}Sr/^{86}Sr$ isotope ratios of Sr single element standard, and (c) Pb isotope ratios of ERM-AE142. Error bars correspond to U (k = 2).

1. IIF per mass unit vs. mass concentration

Figure S10 shows the IIF per mass unit of $^{11}B/^{10}B$, $^{87}Sr/^{86}Sr$ and $^{208}Pb/^{206}Pb$ intensity ratios as a function of mass concentration. For $^{11}B/^{10}B$ the mass concentration range from 100 µg L^{-1} to 5000 µg L^{-1} was investigated, and a maximum extent of IIF per mass unit is observed for mass concentrations between 500 µg L^{-1} and 1000 µg L^{-1}. This does not indicate a correlation between IIF per mass unit and mass concentration. The overall RSD of IIF per mass unit of $^{11}B/^{10}B$ in the mass concentration experiment is 9.4 %, and the overall RSD of $^{11}B/^{10}B$ intensity ratio is 2.1 %. Both RSDs are in the range of the observed within day variation which complicates conclusions regarding possible correlations (compare section 3.3 and Table 1 in the main manuscript). For $^{87}Sr/^{86}Sr$ the mass concentration range from 100 µg L^{-1} to 500 µg L^{-1} was investigated, and a minimum extent of IIF per mass unit was observed for 200 µg L^{-1}. This is not a trend indicating a correlation between IIF per mass unit and mass concentration, but more data points are needed for a more specific statement. The overall RSD of IIF per mass unit of $^{87}Sr/^{86}Sr$ in the mass concentration experiment is 4.4 %, and the overall RSD of $^{87}Sr/^{86}Sr$ intensity ratio is 0.14 %. Both RSDs are in the range of the observed within day variation which makes it complicated to draw conclusions regarding possible correlations (compare section 3.3 and Table 1 in the main manuscript). For $^{208}Pb/^{206}Pb$ the mass concentration range from 100 µg L^{-1} to 2000 µg L^{-1} was investigated, and a minimum extent of IIF per mass unit was observed for 500 µg L^{-1}. Similar to B and Sr, there is no trend indicating a correlation between IIF per mass unit and mass concentration. The overall RSD of IIF per mass unit of $^{208}Pb/^{206}Pb$ in the mass concentration experiment is 5.9 % which is in the range of the observed within day variation which complicates conclusions regarding possible correlations (compare section 3.3 in the main manuscript). The overall RSD of the $^{208}Pb/^{206}Pb$ intensity ratio is 0.43 % which is in the range of the observed within day variation making it complicated to draw conclusions regarding possible correlations (compare Table 1 in the main manuscript). No consistent trend can be observed that could indicate a correlation between mass concentration and the extent of the IIF per mass unit for B, Sr and Pb isotope ratios measured using second generation ICP-TOFMS.

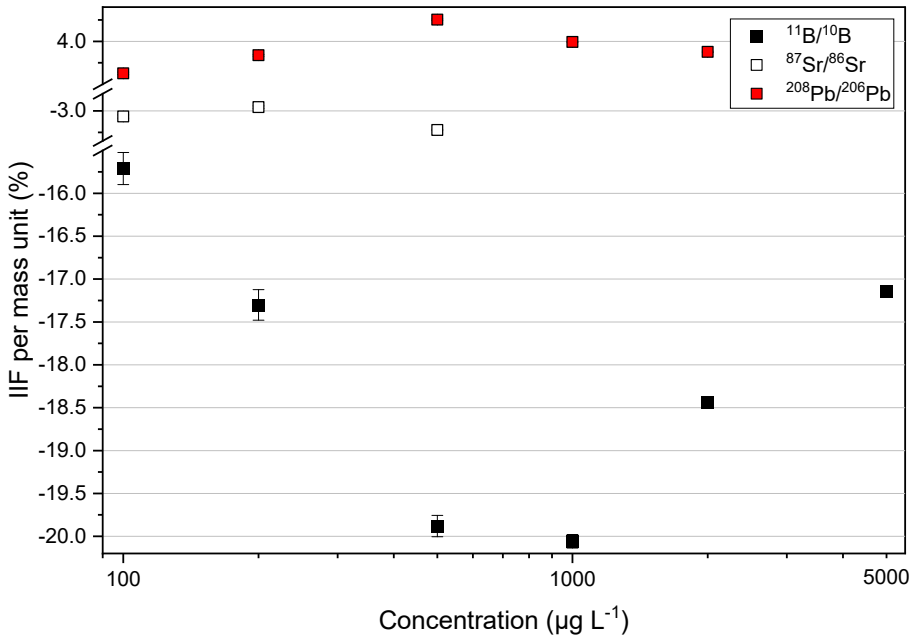

Figure S10 IIF per mass unit (%) of $^{11}B/^{10}B$, $^{87}Sr/^{86}Sr$ and $^{208}Pb/^{206}Pb$ intensity ratios as a function of mass concentration – 100 µg L^{-1} to 5000 µg L^{-1}. Error bars correspond to 2 *s* (acquisition time of 10 s, *M* = 20). The data shown are from the measurement of a mixture in which B, Sr, and Pb were detected simultaneously.

References

1. D. P. Myers and G. M. Hieftje, *Microchem. J.*, 1993, **48**, 259-277.
2. G. M. Hieftje, D. P. Myers, G. Li, P. P. Mahoney, T. W. Burgoyne, S. J. Ray and J. P. Guzowski, *J. Anal. At. Spectrom.*, 1997, **12**, 287-292.
3. P. P. Mahoney, S. J. Ray and G. M. Hieftje, *Appl. Spectrosc.* , 1997, **51**, 16A-28A.
4. F. Vanhaecke, L. Moens, R. Dams, L. Allen and S. Georgitis, *Anal. Chem.*, 1999, **71**, 3297-3303.
5. X. Tian, H. Emteborg and F. C. Adams, *J. Anal. At. Spectrom.*, 1999, **14**, 1807-1814.
6. H. Emteborg, X. Tian, M. Ostermann, M. Berglund and F. C. Adams, *J. Anal. At. Spectrom.*, 2000, **15**, 239-246.
7. R. E. Sturgeon, J. W. H. Lam and A. Saint, *J. Anal. At. Spectrom.*, 2000, **15**, 607-616.
8. X. Tian, H. Emteborg, M. Barbaste and F. C. Adams, *J. Anal. At. Spectrom.*, 2000, **15**, 829-835.
9. M. Barbaste, L. Halicz, A. Galy, B. Medina, H. Emteborg, F. C. Adams and R. Lobinski, *Talanta*, 2001, **54**, 307-317.
10. R. D. Evans, H. Hintelmann and P. J. Dillon, *Journal of Analytical Atomic Spectrometry*, 2001, **16**, 1064-1069.
11. L. Yang, S. Willie and R. E. Sturgeon, *Journal of Analytical Atomic Spectrometry*, 2005, **20**, 1226-1231.
12. A. Saha, V. G. Mishra, S. B. Deb, D. Shah and M. K. Saxena, *Quantification and isotope ratio measurement of boron by ICP-TOF-MS after its pyrohydrolytic extraction from U3Si2-Al fuel*, Indian Society for Mass Spectrometry, India, 2014.
13. A. M. Alvarez, J. R. Estévez Alvarez, C. W. A. do Nascimento, I. P. González, O. D. Rizo, L. L. Carzola, R. A. Torres and J. G. Pascual, *Environ. Monit. Assess.*, 2016, **189**, 28.
14. M. Ohata and H. Hagino, *Int. J. Mass Spectrom.*, 2018, **430**, 31-36.
15. L. Hendriks, A. Gundlach-Graham, B. Hattendorf and D. Günther, *Journal of Analytical Atomic Spectrometry*, 2017, **32**, 548-561.
16. K. G. Heumann, S. M. Gallus, G. Rädlinger and J. Vogl, *J. Anal. At. Spectrom.*, 1998, **13**, 1001-1008.
17. J. Irrgeher and T. Prohaska, in *Sector Field Mass Spectrometry for Elemental and Isotopic Analysis*, eds. T. Prohaska, J. Irrgeher, A. Zitek and N. Jakubowski, The Royal Society of Chemistry, 2015, pp. 107-120.
18. T. Prohaska, J. Irrgeher, J. Benefield, J. K. Böhlke, L. A. Chesson, T. B. Coplen, T. Ding, P. J. H. Dunn, M. Gröning, N. E. Holden, H. A. J. Meijer, H. Moossen, A. Possolo, Y. Takahashi, J. Vogl, T. Walczyk, J. Wang, M. E. Wieser, S. Yoneda, X.-K. Zhu and J. Meija, *Pure and Applied Chemistry*, 2022, **94**, 573-600.
19. CIAAW, Atomic Weights of the Elements, https://www.ciaaw.org/, 2023).